JHEP

Published for SISSA by Springer

Received: August 30, 2014
Revised: November 20, 2014
Accepted: December 2, 2014
Published: December 18, 2014

Hint of lepton flavour non-universality in B meson decays

Diptimoy Ghosh,[a] **Marco Nardecchia**[b] **and S.A. Renner**[b]

[a] *INFN — Sezione di Roma, Piazzale A. Moro 2, I-00185 Roma, Italy*

[b] *DAMTP, University of Cambridge, Wilberforce Road, Cambridge CB3 0WA, U.K.*

E-mail: diptimoy.ghosh@roma1.infn.it, m.nardecchia@damtp.cam.ac.uk, sar67@cam.ac.uk

Abstract: The LHCb collaboration has recently presented their result on $R_K = \mathcal{B}(B^+ \to K^+\mu^+\mu^-)/\mathcal{B}(B^+ \to K^+e^+e^-)$ for the dilepton invariant mass bin $m^2_{\ell\ell} = 1 - 6$ GeV^2 ($\ell = \mu, e$). The measurement shows an intriguing $2.6\,\sigma$ deviation from the Standard Model (SM) prediction. In view of this, we study model independent New Physics (NP) explanations of R_K consistent with other measurements involving $b \to s\,\ell^+\,\ell^-$ transition, relaxing the assumption of lepton universality. We perform a Bayesian statistical fit to the NP Wilson Coefficients and compare the Bayes Factors of the different hypotheses in order to quantify their goodness-of-fit. We show that the data slightly favours NP in the muon sector over NP in the electron sector.

Keywords: Rare Decays, Beyond Standard Model, B-Physics

ArXiv ePrint: 1408.4097

doi:10.1007/JHEP12(2014)131

Contents

1 Introduction 1

2 Effective field theory approach 2

3 Results 3
- 3.1 Single Wilson coefficient 4
- 3.2 Combination of two Wilson coefficients at a time 6
- 3.3 Including the data on $B \to K^* \mu^+ \mu^-$ 8

4 Summary and conclusions 9

A Details of the analysis 11
- A.1 $B^+ \to K^+ \ell^+ \ell^-$ 11
- A.2 R_K 12
- A.3 $B \to X_s \, \ell^+ \, \ell^-$ 12
- A.4 $B_s \to \ell^+ \, \ell^-$ 12

B Statistical procedure 13

C Input parameters 14

JHEP12(2014)131

1 Introduction

While we all hope to see direct evidence of new particles in the upcoming 14 TeV run of the LHC, indirect searches for New Physics (NP) through precision measurements are also extremely important, in particular because of their high sensitivity to Ultra Violet (UV) physics. In fact, the 8 TeV run of the LHC has already seen interesting indirect hints of NP in some of the B meson decay modes. The quoted 3.7 σ deviation observed by the LHCb collaboration last summer [1, 2] in one of the angular observables (P_5') in the decay $B \to K^* \mu^+ \mu^-$ for one of the dilepton invariant mass bins ($4.30 < q^2 = m^2_{\mu\,\mu} < 8.68$ GeV^2) inspired many theorists to come up with NP explanations [3–10]. Interestingly enough, very recently the LHCb collaboration has observed a 2.6σ deviation in another $b \to s \, \ell^+ \, \ell^-$ mode; in the quantity called R_K which is the ratio of the two branching fractions $\mathcal{B}\,(B^+ \to K^+ \mu^+ \mu^-)$ and $\mathcal{B}\,(B^+ \to K^+ e^+ e^-)$ in the dileptonic invariant mass bin $m^2_{\ell\,\ell} = 1 - 6\,\text{GeV}^2$ ($\ell = \mu, e$) [11]. Note that the branching ratios $\mathcal{B}\,(B^+ \to K^+ \mu^+ \mu^-)$ and $\mathcal{B}\,(B^+ \to K^+ e^+ e^-)$ are individually predicted with very large hadronic uncertainties ($\sim 30\%$) in the SM [12]. However, their ratio is a theoretically very clean observable and predicted to be $R_K^{\rm SM} = 1$ if lepton masses are ignored [13]. Inclusion of the lepton mass effects changes the prediction only by a tiny amount making it $R_K^{\rm SM} = 1.0003 \pm 0.0001$ [12].

This is in contrast to the (P_5') anomaly where considerable debate exists surrounding the issue of theoretical uncertainty due to (unknown) power corrections to the factorization framework [14–16]. Hence, there is a possibility that the observed deviation might be (partly) resolved once these corrections are better understood. On the other hand, the observable R_K is a ratio of two branching fractions which differ only in the flavour of the final state leptons. This makes R_K well protected from hadronic uncertainties in the SM because the strength of the gauge interactions contributing to the short distance physics in the $b \to s\,\ell^+\,\ell^-$ transition are independent of the final state lepton flavour. In fact, this feature remains true even in NP models if the model respects lepton universality. Therefore, the R_K measurement is perhaps pointing towards new short distance physics which is not lepton universal. This motivated us to study possible NP explanations of the R_K measurement (and their consistency with other observables involving the $b \to s\,\ell^+\,\ell^-$ transition) in a model independent way, relaxing the assumption of lepton universality. To this end, we perform a statistical fit to the NP Wilson Coefficients (WC) employing Bayesian inference. In order to quantify and compare the goodness-of-fit of the different hypotheses we also compute their relative Bayes Factors (BFs).

The paper is organized as follows. In the next section we set up our notation and discuss all the experimental data used in our analysis. We present our results in section 3 and conclude with some final remarks in section 4.

2 Effective field theory approach

We base our analysis on the following $|\Delta B| = |\Delta S| = 1$ effective Hamiltonian,

$$\mathcal{H}_{\rm eff} = -\frac{4G_F}{\sqrt{2}}\,(V_{ts}^* V_{tb})\,\sum_i \hat{C}_i^\ell(\mu)\,\mathcal{O}_i^\ell(\mu)\ , \tag{2.1}$$

where $\mathcal{O}_i^\ell$ are the $\mathrm{SU(3)_C} \times \mathrm{U(1)_Q}$ invariant dimension-six operators responsible for the flavour changing $b \to s\,\ell^+\,\ell^-$ transition. The superscript ℓ denotes the lepton flavour in the final state ($\ell = e, \mu$). In our notation the short-distance contribution to the WCs is divided into the SM and the NP ones in the following way $\hat{C}_i^\ell = C_i^{\rm SM} + C_i^\ell$. In our analysis we consider the subset of operators which are directly responsible for the $b \to s\,\ell^+\,\ell^-$ decay, namely

$$\mathcal{O}_7 = \frac{e}{16\pi^2}\,m_b\,(\bar{s}\sigma_{\alpha\beta}P_R b)\,F^{\alpha\beta}\ , \tag{2.2}$$

$$\mathcal{O}_9^\ell = \frac{\alpha_{\rm em}}{4\pi}\,(\bar{s}\gamma_\alpha P_L b)\,(\bar{\ell}\gamma^\alpha \ell)\ , \tag{2.3}$$

$$\mathcal{O}_{10}^\ell = \frac{\alpha_{\rm em}}{4\pi}\,(\bar{s}\gamma_\alpha P_L b)\,(\bar{\ell}\gamma^\alpha\gamma_5 \ell) \tag{2.4}$$

and the set of chirality flipped operators $\mathcal{O}_i'$ obtained by interchanging the chiral projectors ($P_L \leftrightarrow P_R$) in the quark current of $\mathcal{O}_i$. The full list of dimension six operators also includes scalar, pseudo-scalar and tensor structures. However, it has been shown that scalar, pseudo-scalar and tensor operators cannot easily give sufficiently large deviations from the SM in the observable R_K once constraints from the other $b \to s\,\ell^+\,\ell^-$ processes are taken into

JHEP12(2014)131

Observable	SM prediction		Measurement	
$\mathcal{B}\left(B^+ \to K^+\mu^+\mu^-\right)_{[1,6]}$	$\left(1.75^{+0.60}_{-0.29}\right) \times 10^{-7}$	[19]	$(1.21 \pm 0.09 \pm 0.07) \times 10^{-7}$	[20]
$\mathcal{B}\left(B^+ \to X_s\mu^+\mu^-\right)_{[1,6]}$	$(1.59 \pm 0.11) \times 10^{-6}$	[21]	$\left(0.66^{+0.82+0.30}_{-0.72-0.24} \pm 0.07\right) \times 10^{-6}$	[22]
$\mathcal{B}\left(B_s \to \mu^+\mu^-\right)$	$(3.65 \pm 0.23) \times 10^{-9}$	[23]	$(2.9 \pm 0.7) \times 10^{-9}$	[24]
$\mathcal{B}\left(B^+ \to X_s e^+e^-\right)_{[1,6]}$	$(1.64 \pm 0.11) \times 10^{-6}$	[21]	$\left(1.93^{+0.47+0.21}_{-0.45-0.16} \pm 0.18\right) \times 10^{-6}$	[22]
$\mathcal{B}\left(B_s \to e^+e^-\right)$	$(8.54 \pm 0.55) \times 10^{-14}$	[23]	$< 2.8 \times 10^{-7}$	[25]
$R_{K\,[1,6]}$	1.0003 ± 0.0001	[12]	$0.745^{+0.090}_{-0.074} \pm 0.036$	[11]

Table 1. The observables used in our analysis along with their SM predictions and experimental measurements.

account [17, 18]. Therefore, we will neglect these operators in our analysis. Furthermore, we do not consider NP contributions to the photonic dipole operator $\mathcal{O}_7$ as it is lepton flavour blind by construction. In what follows we assume that all the WCs are evaluated at the scale $\mu = m_b$ with the corresponding SM contributions given in table 5.

Apart from R_K we also consider data for other processes which proceed via a $b \to s\,\ell^+\,\ell^-$ transition e.g., the branching ratios of the fully leptonic decays $B_s \to \mu^+\mu^-$ and $B_s \to e^+e^-$, the inclusive decays $B \to X_s\mu^+\mu^-$ and $B \to X_s e^+e^-$ as well as the branching ratio for the semileptonic decay $B^+ \to K^+\mu^+\mu^-$. The SM predictions for these branching fractions and their current experimental values are summarized in table 1. Note that the experimental upper bound on $\mathcal{B}(B_s \to e^+e^-)$ is larger than the SM prediction by many orders of magnitude. We include this decay mode for completeness but it has no impact on our final results.

We have not used the branching fraction for the decay $B^+ \to K^+e^+e^-$ from [11] because of its correlation with the R_K measurement. Instead, we have used the value of $\mathcal{B}(B^+ \to K^+\mu^+\mu^-)$ from a LHCb measurement in [20]. Moreover, we have used the data for $\mathcal{B}(B^+ \to K^+\mu^+\mu^-)$ only in the low-q^2 bin $1 - 6\,\text{GeV}^2$, the main reason being that a resonance structure in the dilepton invariant mass distribution was observed around $m^2_{\mu\,\mu} = 17.3\,\text{GeV}^2$ by the LHCb collaboration last year [26]. This means that even though form factors in the high-q^2 region were recently computed from lattice QCD [27–30], the theoretical prediction for this observable is affected by non-factorisable hadronic uncertainties. Information coming from high-q^2 measurements of this and other observables (such as $\mathcal{B}(B_s \to \phi\mu^+\mu^-)$, $\mathcal{B}(\overline{B}^0 \to \overline{K}^0\mu^+\mu^-)$, etc.) can still be used taking into account conservative estimates of the hadronic uncertanties. We do not expect that the inclusion of such data would change our results drastically, however we expect that the allowed ranges of the WCs would shrink due to the extra observables. We also expect a shift of the best fit points in the direction of the SM values, since these extra measurements are generally in good agreement with the SM predictions.

3 Results

In this section we present our results for the various NP scenarios considered in this paper. As mentioned earlier, we follow a Bayesian statistical approach to quantify our results. The details of our procedure is explained in the appendix B.

JHEP12(2014)131

3.1 Single Wilson coefficient

To start with, we consider only one real NP WC at a time. We will show our results for the WCs both in the standard basis (vector and axial-vector operators for the lepton current) as well as in the chiral basis for the lepton currents. The inclusion of the second set is motivated by the possibility of having the NP WCs generated in an $SU(2)_L$ invariant way. This possibility was also highlighted in [18].

Our results are summarized in table 2. The 68% confidence level (C.L.) regions of the WCs are shown in the second column, the best fit values are shown in the third column while the last column shows the BF for each hypothesis taking the same for the C_9^μ-only hypothesis as the reference value. More precisely, the BF for the hypothesis with NP in the WC C_i^ℓ is defined as

$$\mathrm{BF}(C_i^\ell) = \frac{\int \mathcal{L}\left(\mathrm{data}|C_i^\ell\right) \times P_0(C_i^\ell)\, dC_i^\ell}{\int \mathcal{L}\left(\mathrm{data}|C_9^\mu\right) \times P_0(C_9^\mu)\, dC_9^\mu}\,, \tag{3.1}$$

where $\mathcal{L}$ is the likelihood function and P_0 is our choice of prior for the WC C_i^ℓ, which we assume to be a flat distribution in the range [-10, 10].

In figure 1 we show the posterior probabilities for the C_9^μ only and C_9^e only hypotheses as examples.

We now discuss some general features of our results shown in table 2. Clearly, the hypothesis with non-zero C_9^μ is the most favoured by the data as it offers the largest BF. The C_{10}^μ NP scenario also does quite well. As $C_9^{\mu\prime}$ does not contribute to the decay $B_s \to \mu^+\mu^-$ (whose experimental central value is now slightly lower than the SM prediction), its BF is reduced to some extent. The extremely low BF for the $C_{10}^{\mu'}$ case is due to a tension between R_K and and $\mathcal{B}(B_s \to \mu^+\mu^-)$. It can be seen from the expressions of these two observables (see appendices A.1 and A.4) that the experimental value for R_K prefers $C_{10}^{\mu'} > 0$ while the measured branching ratio for $B_s \to \mu^+\mu^-$ prefers the opposite. The hypotheses $C_9^{\mu(\prime)} = C_{10}^{\mu(\prime)}$ (which correspond to the operator directions $(\bar{s}\gamma_\alpha P_L b)(\bar{\ell}\gamma^\alpha P_R \ell)$ and $(\bar{s}\gamma_\alpha P_R b)(\bar{\ell}\gamma^\alpha P_R \ell)$) are also strongly disfavoured because they generate $R_K \gtrsim 1$ which is in tension with experiment. The other chiral operator $(\bar{s}\gamma_\alpha P_L b)(\bar{\ell}\gamma^\alpha P_L \ell)$ (our hypothesis $C_9^\mu = -C_{10}^\mu$) turns out to be the best among the four chiral operators. This case was also considered in ref. [18] in the context of their model independent analysis as well as a specific leptoquark model. In their analysis they quote $C_9^\mu = -C_{10}^\mu \approx -0.5$ as a benchmark point which is in fact consistent with our 68% CL range in table 2.

As far as NP in the electron sector is concerned, all the hypotheses give similar BFs (at most a factor 4 between the best and the worst). This can be understood by the fact that the measurements with electrons in final states have a larger experimental error than those with muons in the final state. Note also that there are a few cases with multiple solutions (because the rates are quadratically dependent on the WCs), some of them with very large NP contributions (see for example C_{10}^e). Including other observables (for example those in the decay $B \to K^*\ell^+\ell^-$) will certainly modify this picture.

The scenario $C_{10}^{e'} = -C_9^{e'} \approx 0.5$ was also considered in the ref. [18]. Although their estimate $C_{10}^{e'} \approx 0.5$ is compatible with the 68% CL region from our fit, its BF is the worst among the hypotheses with NP in the electron sector.

JHEP12(2014)131

Hypothesis	Fit	Best fit	BF
C_9^μ	[-3.1,-0.7]	-1.6	1 : 1
$C_9^{\mu'}$	[-1.9,-0.8]	-1.3	0.20 : 1
C_{10}^μ	[0.7,1.3], [7.5,8.1]	1.0	0.82 : 1
$C_{10}^{\mu'}$	[0.2,0.7]	0.5	4.8×10^{-3} : 1
$C_9^\mu = +C_{10}^\mu$	[0.1,0.8]	0.5	2.7×10^{-3} : 1
$C_9^\mu = -C_{10}^\mu$	[-0.8,-0.4]	-0.6	0.42 : 1
$C_9^{\mu'} = +C_{10}^{\mu'}$	[-0.4,0.3]	-0.1	9.3×10^{-4} : 1
$C_9^{\mu'} = -C_{10}^{\mu'}$	[-0.2,-0.6]	-0.4	1.3×10^{-2} : 1
C_9^e	[-8.4,-8.4], [0.6,2.1]	1.3	0.13 : 1
$C_9^{e'}$	[0.8,1.9]	1.3	0.10 : 1
C_{10}^e	[-1.6,-0.7], [9.5,10.0]	-1.1	0.14 : 1
$C_{10}^{e'}$	[-1.7,-0.7]	-1.1	9.7×10^{-2} : 1
$C_9^e = +C_{10}^e$	[-2.4,-1.4], [2.2,3.4]	-1.9	0.20 : 1
$C_9^e = -C_{10}^e$	[0.3,1.1]	0.6	6.7×10^{-2} : 1
$C_9^{e'} = +C_{10}^{e'}$	[-2.6,-1.5], [2.2,3.2]	-2.0	0.20 : 1
$C_9^{e'} = -C_{10}^{e'}$	[0.4,0.9]	0.7	5.2×10^{-2} : 1
C_9^μ=C_9^e	[-4.3,-1.1]	-2.2	2.9×10^{-2} : 1
C_{10}^μ=C_{10}^e	[0.3,1.2], [7.6,8.4]	0.8	1.7×10^{-2} : 1
SM			2.4×10^{-3} : 1

Table 2. The 68% C.L. ranges for the WCs when only one WC is considered at a time. The data on $B \to K^* \mu^+ \mu^-$ have not been used at this stage.

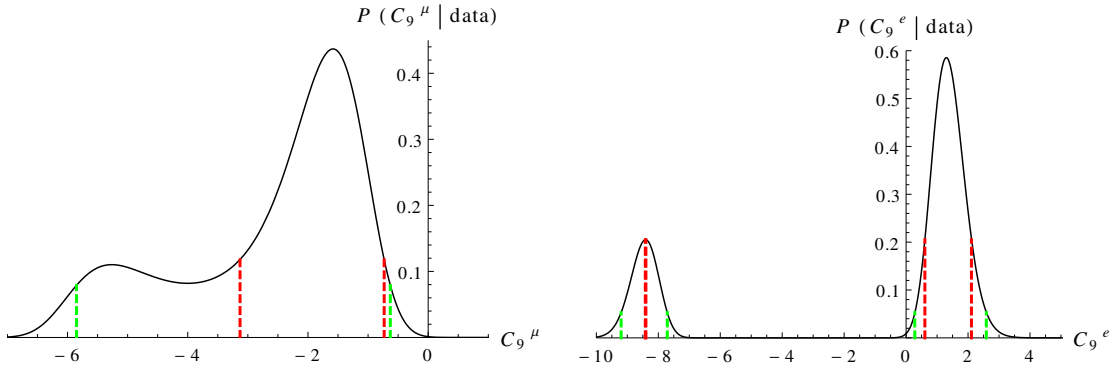

Figure 1. Posterior probabilities for the C_9^μ only (left) and C_9^e only (right) hypotheses. The red and green vertical lines refer to boundaries of 68% and 95% regions respectively.

The highest BFs are obtained for hypotheses with NP in the muon sector. In our fit, this finding is driven by the observables $\mathcal{B}(B \to X_s \ell^+ \ell^-)$ and $\mathcal{B}(B^+ \to K^+ \mu^+ \mu^-)$, for which the dimuon channel measurements are each lower (at more than 1σ level) than the

JHEP12(2014)131

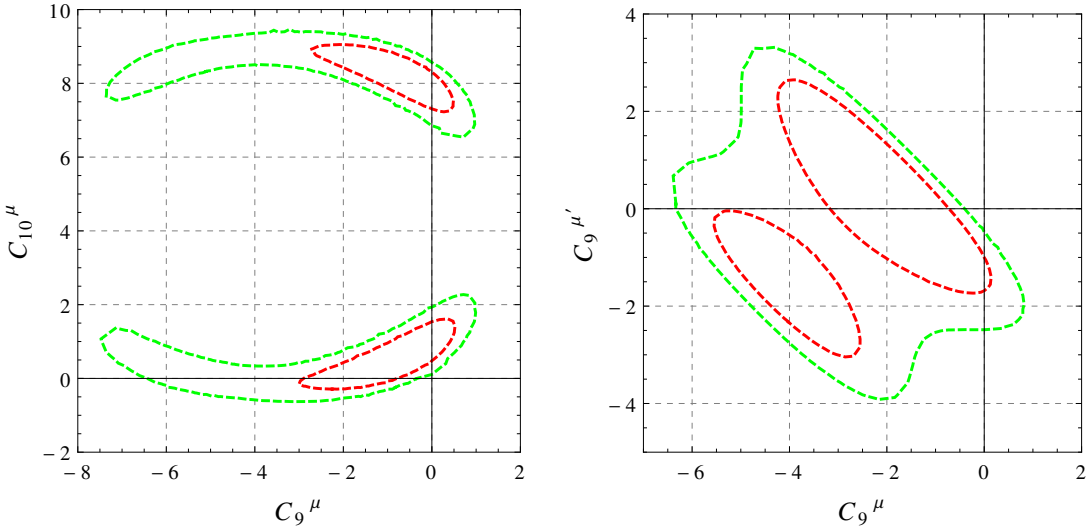

Figure 2. Two dimensional posterior probability distributions for the two hypotheses: 1. C_9^μ and C_{10}^μ (left panel), 2. C_9^μ and $C_9^{\mu\prime}$ (right panel). The red and green contours are 68% and 95% C.L. regions respectively.

SM predictions, while the electron channel measurement is in good agreement with the SM. Hence our fit finds a slight preference for NP in the muon sector. For example, a negative value for C_9^μ will lower the predictions for both $\mathcal{B}(B \to X_s\mu^+\mu^-)$ and $\mathcal{B}(B^+ \to K^+\mu^+\mu^-)$ compared to the SM while keeping $\mathcal{B}(B \to X_s e^+e^-)$ at its SM value.

Finally, we show our results for the two lepton universal cases $C_9^\mu{=}C_9^e$ and $C_{10}^\mu{=}C_{10}^e$ (see the last but one row in table 2). It can be seen that the BF for both these two cases are rather low compared to most of the non-universal NP scenarios in particular, the C_9^μ-only and C_{10}^μ-only hypotheses.

3.2 Combination of two Wilson coefficients at a time

In this section we allow the possibility of having NP in two WCs simultaneously and study the consequences. Here we do not consider all the possible combinations of the WCs, rather, we take the few best cases from table 2 and consider their combinations. Our results are summarized in table 3. The 68% range of a parameter is obtained after marginalizing over the other parameter.

The results of our analysis show that, in general, there is no particular gain in considering NP effects in two WCs at the same time, this is more marked in the case of the chiral operators.

Among the hypothesis of NP in two WCs, the largest BF is obtained for the pair $\{C_9^e, C_9^\mu\}$. The 2-dimensional posterior distribution for this scenario is shown in the left panel of figure 2. Similarly, the posterior probability distribution for the NP scenario with both C_9^μ and $C_9^{\mu\prime}$ is shown is the right panel of figure 2. It can be seen that the data is consistent with no NP in $C_9^{\mu\prime}$.

The posterior probability for the hypothesis with both C_9^μ and C_9^e turned on is shown in figure 3. In the left panel we show both the allowed regions, while in the right panel

JHEP12(2014)131

Hypothesis	Fit	Best fit	BF
C_9^μ	[-1.9,0.3]	-0.6	0.15 : 1
C_{10}^μ	[-0.1,0.9], [8.0,8.8]	0.4	
C_9^μ	[-4.2,-1.2]	-2.8	0.20 : 1
$C_9^{\mu'}$	[-1.7,1.2]	-0.3	
C_9^μ	[-4.2,-1.4]	-2.6	0.28 : 1
C_9^e	[-7.4,-5.9], [-1.3,0.2]	-6.6	
$C_9^\mu = -C_{10}^\mu$	[-1.0,0.4]	-0.7	4.5×10^{-2} : 1
$C_9^e = -C_{10}^e$	[-0.5,0.4], [-8.2,-7.4]	-0.1	
$C_9^\mu = -C_{10}^\mu$	[-0.7,-0.4]	-0.5	8.3×10^{-2} : 1
$C_9^e = C_{10}^e$	[-1.2,1.6]	-0.2	
$C_9^\mu = C_{10}^\mu$	[0.1,0.9]	0.5	8.0×10^{-3} : 1
$C_9^e = -C_{10}^e$	[0.3,1.1]	0.6	
$C_9^\mu = C_{10}^\mu$	[0.1,0.9]	0.5	2.4×10^{-2} : 1
$C_9^e = C_{10}^e$	[-2.4,-1.5], [2.2,3.4]	2.8	

Table 3. Same as table 2 but with two WCs turned on simultaneously.

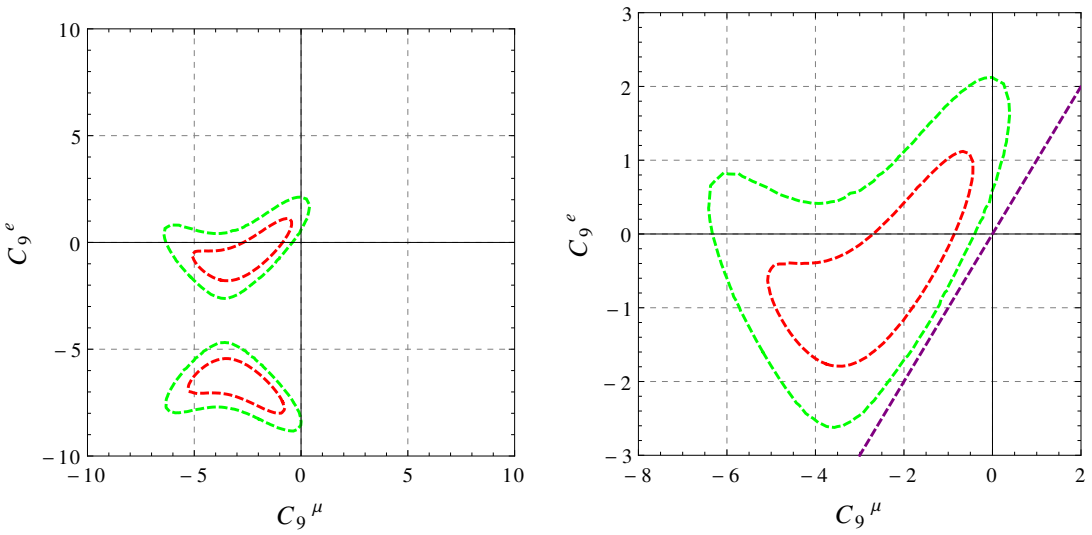

Figure 3. Two dimensional posterior probability distribution for the hypothesis with NP in C_9^μ and C_9^e. In the left panel both the allowed regions are shown. In the right panel we show only the region close to the origin. The red and green contours are 68% and 95% C.L. regions respectively. The purple line represents the lepton flavour universal scenario $C_9^\mu = C_9^e$.

we show a zoomed in version of the region close to the SM point $C_9^\mu = C_9^e = 0$. Figure 3 clearly shows that the data prefers NP in the muon sector over NP in the electron sector. Moreover, NP with lepton flavour universality (shown by the the dashed purple line) is disfavoured by more than 95% C.L.

JHEP12(2014)131

Hypothesis	Fit	Best Fit	BF
C_9^μ	[-1.9,-1.3]	-1.6	1 : 1
C_9^μ	[-1.9,-1.3]	-1.6	0.14 : 1
C_9^e	[-7.7,-6.6], [-0.7,0.6]	-0.1	
C_9^μ	[-1.8,-1.4]	-1.6	0.13 : 1
C_{10}^e	[-0.4,0.5], [8.3,9.3]	8.7	
C_9^μ	[-1.8,-1.3]	-1.5	0.16 : 1
$C_9^e = C_{10}^e$	[-0.9,1.5]	-0.1	
C_9^μ	[-1.9,-1.3]	-1.6	6.0×10^{-2} : 1
$C_9^e = -C_{10}^e$	[-8.2,-7.8], [-0.3,0.3]	0.0	

Table 4. Results when the data on $B \to K^* \mu^+ \mu^-$ are also included as discussed in section 3.3. The same conventions as in table 2 and 3 are used.

3.3 Including the data on $B \to K^* \mu^+ \mu^-$

The latest LHCb measurement of the decay distribution in $B \to K^* \mu^+ \mu^-$ has seen interesting deviations in several observables from their SM predictions [1, 2]. These deviations were most pronounced in two of the so-called optimized observables (where the hadronic uncertainties are expected to cancel to a good extent) P_5' and P_2' in the low-q^2 region [31]. Soon after the LHCb result was published, it was shown in [3] that a good fit to all the data can be obtained by having a negative contribution in the range $[-1.9, -1.3]$ to the WC $\hat{C}_9^\mu$. A similar conclusion was also reached by two other groups [4, 32]. The fit done in [4] found a need for a NP contribution (similar to C_9^μ in magnitude but with opposite sign) also to the chirally flipped operator $\hat{C}_9^{\mu\prime}$. As discussed in section 3.2 this is now in tension with the measurement of R_K (assuming the presence of NP only in the muon sector).

Note that the issue of hadronic uncertainties, in particular the role of long-distance $c\bar{c}$ loops still remains unclear, see [16] and the references therein for a recent discussion. Thus, the jury is still out on whether NP has already been seen in these measurements. Despite this uncomfortable situation, several NP interpretations of the LHCb data have been proposed [6–8] and it would be interesting to see whether the R_K measurement can be reconciled with the $B \to K^* \mu^+ \mu^-$ data. With this motivation, in this section we combine the result of [3] with our analysis.

We follow an approximate procedure (see appendix B for more details) which allows us to use their result where NP only in $\hat{C}_9^\mu$ and $\hat{C}_7$ was considered, see their eq. 4. Note that, although the analysis in [3] was performed assuming lepton universality their results can, to a very good approximation, be taken as valid only for the muonic WCs. This allows us to safely use their result with NP in $\hat{C}_9^\mu$ and any operator in the electron sector. As we do not consider NP in the dipole operator in this paper, $\hat{C}_7$ is set to its SM value (which is consistent with the 68% C.L. region of [3]).

The result of our fit is reported in table 4. In the first row we show the result when only C_9^μ is turned on while in the following rows we allow NP in the electron sector in addition

JHEP12(2014)131

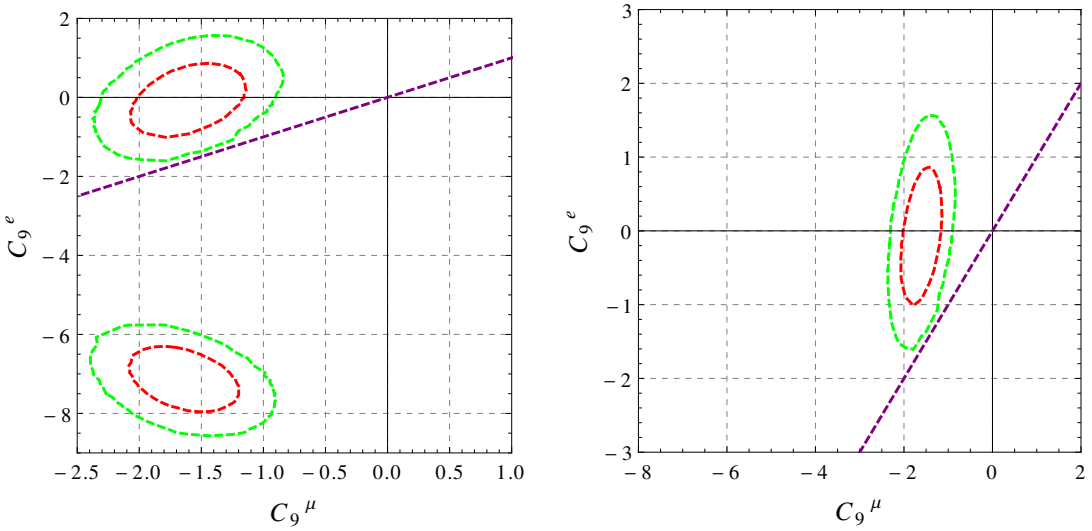

Figure 4. Two dimensional posterior probability distributions for the hypothesis C_9^μ–C_9^e including the data on $B \to K^* \mu^+ \mu^-$ (see text for more details). The same conventions as in figure 3 are used.

to C_9^μ. We notice that the range for C_9^μ preferred by the analysis of [3] is confirmed even with the inclusion of our observables. Allowing the possibility of NP in the electron sector makes things slightly better (increases the BF by roughly a factor of 3), except for the scenario of the last row of the table where the BF remains almost the same. The posterior probability distribution for the C_9^μ - C_9^e hypothesis is shown in figure 4. Similar to figure 3, in the left panel both the allowed regions are shown while in the right panel only the region close to the SM point is shown. Again, the preference for lepton flavour non-universal NP is very clear. The data is consistent with no NP in the electron sector but demands a rather large NP in the muon sector. A comparison of the figure in the right panel with that in figure 3 will also show the constraining power of the $B \to K^* \mu^+ \mu^-$ data. We warn the readers that the BFs in the table 4 should not be compared with those in the previous section but should only be compared within table 4. This is because the analysis in this section uses different set of information than those in the previous section. Also, we are combining our analysis with that in [3] in a very simplified way. We report the BFs just to show that the data does not show a strong preference for any particular kind of NP in the electron sector; many of them do equally well.

4 Summary and conclusions

The flavour changing process $b \to s\, \ell^+ \ell^-$ is responsible for many rare decays such as $B_s \to \ell^+ \ell^-$, $B \to X_s \ell^+ \ell^-$, $B^+ \to K^+ \ell^+ \ell^-$ and $B \to K^* \ell^+ \ell^-$. These decays, being extremely rare in the SM, are very powerful probes of NP. The LHCb collaboration already made significant progress last year by measuring most of the observables in the full three angle distribution of the decay $B \to K^* \mu^+ \mu^-$. Interesting deviations from the SM predictions were seen in a few of the so-called "form-factor independent" or optimized observables.

JHEP12(2014)131

Although several NP explanations of these deviations were put forward, firm confirmation of NP in these observables is not yet possible due to the hadronic uncertainties which are not completely understood. The 2.6σ deviation in R_K, although not yet statistically significant, is worthy of attention because the ratio R_K is essentially free of hadronic uncertainties in the SM. Moreover, any lepton flavour blind new short distance physics would predict $R_K \approx R_K^{\rm SM}$ and hence, the confirmation of this deviation would clearly point towards lepton flavour non-universal NP. This has motivated us to study model independent NP explanations of the measurement of R_K considering various observables involving a $b \to s\,\ell^+\,\ell^-$ transition. To this end, we have performed a Bayesian statistical analysis of the various NP scenarios. We have also quantified the goodness-of-fit of these NP hypotheses by computing and comparing their Bayes Factors.

We first performed a fit without including the data on $B \to K^*\mu^+\mu^-$. Our results for the hypothesis of NP in one (two) WC(s) at a time are summarized in table 2 (3). In the muon sector, among the fits to a single WC in the standard basis, only C_9^μ and C_{10}^μ have large BFs while among the chiral operators, the hypothesis of NP in $C_9^\mu = -C_{10}^\mu$ gives the highest BF. In the electron sector all the NP hypotheses give comparable BFs, although worse than the scenarios with C_9^μ or C_{10}^μ. Even without the inclusion of the $B \to K^*\mu^+\mu^-$ data, our fit shows a slight preference towards the hypothesis of NP in the di-muon sector. However it should be noted that large NP effects in the electron sector are not excluded and in the future, with more precise measurements, the situation could change. We further show that the lepton flavour universal NP scenarios for example, $C_9^\mu = C_9^e$ or $C_{10}^\mu = C_{10}^e$ have rather low BFs and hence they are disfavoured.

When two NP WCs are turned on simultaneously, the situation does not particularly improve. We have shown a few posterior distributions in figures 2 and 3 and we notice that for the C_9^μ–C_9^e hypothesis the lepton flavour universal case $C_9^\mu = C_9^e$ is disfavoured at more than 95% C.L. We continued in section 3.3 by including also the data on $B \to K^*\mu^+\mu^-$. We employed a simplified procedure (explained in appendix B) to combine part of the results from [3] with our observables. We observed that the allowed range of C_9^μ obtained in [3] remains consistent with the R_K data. Our analysis also showed that the data is consistent with no NP in the electron sector.

A global analysis including the final states with tau leptons would be very interesting once more data are available. In fact, the possibility of large enhancements in many of the $b \to s\tau^+\tau^-$ modes were already discussed in the context of like-sign dimuon asymmetry seen at the Tevatron, see for example [33, 34].

Acknowledgments

DG is supported by the European Research Council under the European Union's Seventh Framework Programme (FP/2007-2013) / ERC Grant Agreement n.279972. DG would like to thank Prof. Benjamin Allanach for his hospitality in DAMTP, University of Cambridge where this project was envisaged. DG also thanks Prof. Michael Spannowsky and the CERN theory division for their hospitalities in IPPP Durham and CERN respectively where part of this work was carried out. Discussion with Prof. Luca Silvestrini is also

JHEP12(2014)131

gratefully acknowledged. MN and SR are supported by STFC. MN and SR want to thank Ben Allanach for useful discussions on Bayesian statistics. Thanks to Diego Guadagnoli and David Straub for helpful comments.

A Details of the analysis

A.1 $B^+ \to K^+\ell^+\ell^-$

The branching ratio for the decay $B^+ \to K^+\ell^+\ell^-$ in the low-q^2 region can be written as [12, 35–37],

$$\begin{aligned}\mathcal{B}\left(B^+ \to K^+\ell^+\ell^-\right)_{[1,6]} = & \frac{\tau_B^{\pm} G_F^2 \alpha_e^2 \left|V_{tb}V_{ts}^*\right|^2}{2^9\pi^5 m_{B^\pm}^3}\frac{1}{3} \\ & \times\Bigg(\left|C_{10}^{\rm SM} + C_{10}^{\ell} + C_{10}^{\ell'}\right|^2 (f_{BK}^+)^2 \left(I_1 + 2I_2\, b_1^+ + I_3 (b_1^+)^2\right) \\ & + \left|C_9^{\rm SM} + C_9^{\ell} + C_9^{\ell'}\right|^2 (f_{BK}^+)^2 \left(I_1 + 2I_2\, b_1^+ + I_3 (b_1^+)^2\right) \\ & + \left|C_7^{\rm SM}\right|^2 (f_{BK}^T)^2 \left(I_1 + 2I_2\, b_1^T + I_3 (b_1^T)^2\right) \left(\frac{2m_b}{m_{B^\pm} + m_{K^\pm}}\right)^2 \\ & + {\rm Re}\left[C_7^{\rm SM}(C_9^{\rm SM} + C_9^{\ell} + C_9^{\ell'})^*\right] \\ & \times f_{BK}^+ f_{BK}^T \left(I_1 + I_2\,(b_1^+ + b_1^T) + I_3 b_1^+ b_1^T\right) \frac{4m_b}{m_{B^\pm} + m_{K^\pm}}\Bigg)\,, \end{aligned} \tag{A.1}$$

where the numerical values for I_1, I_2 and I_3 are given by,

$$\begin{aligned} I_1 &= 89729.8\,, \\ I_2 &= -2703.44\,, \\ I_3 &= 97.3014\,. \end{aligned}$$

In order to obtain these numbers we have used the form factor parametrization given in [37]. The values of the form factor parameters f_{BK}^+, f_{BK}^T, b_1^+ and b_1^T are given in table 5. As far as the uncertainties in these parameters are concerned, for b_1^+ and b_1^T we have taken asymmetric gaussian priors in the fit. For the other two parameters f_{BK}^+ and f_{BK}^T, we have fixed them to their respective central values and the associated uncertainties are taken into account by rescaling the experimental error $\sigma_{\mathcal{B}}$ in $\mathcal{B}\left(B^+ \to K^+\mu^+\mu^-\right)_{[1,6]}$ by

$$\sigma_{\mathcal{B}} \to \sqrt{\sigma_{\mathcal{B}}^2 + 4\frac{\sigma_f^2}{f_{BK}^2}\overline{\mathcal{B}}^2} = 0.37 \times 10^{-7} \tag{A.2}$$

(taking conservatively the values $f_{BK} = 0.34$, $\sigma_f = 0.05$ and $\overline{\mathcal{B}} = 1.21 \times 10^{-7}$) . We made this (conservative) approximation in order to reduce the computational time in the evaluation of the posterior distributions for the WCs and avoid some numerical instabilities. We have followed the same prescription also for the branching ratio of $B^+ \to K^+e^+e^-$. The theoretical uncertainties coming from f_{BK}^+ and f_{BK}^T in the two observables $\mathcal{B}(B^+ \to K^+\mu^+\mu^-)$ and $\mathcal{B}(B^+ \to K^+e^+e^-)$ have been assumed to be independent for simplicity.

JHEP12(2014)131

A.2 R_K

The expression for R_K can be derived using the result given in the previous subsection. Here we give a simplified formula which can be useful for analytic understanding of our results. Observing the fact that $\left|\frac{C_7^{\rm SM}}{C_{9,10}^{\rm SM}}\right| \approx 0.07$ and also that the NP in $\hat{C}_7$ is severely constrained by the measured branching ratio of $B \to X_s\gamma$, the expression of R_K can be approximated by,

$$R_K \approx \frac{\left|C_{10}^{\rm SM} + C_{10}^{\mu} + C_{10}^{\mu'}\right|^2 + \left|C_9^{\rm SM} + C_9^{\mu} + C_9^{\mu'}\right|^2}{\left|C_{10}^{\rm SM} + C_{10}^{e} + C_{10}^{e'}\right|^2 + \left|C_9^{\rm SM} + C_9^{e} + C_9^{e'}\right|^2}\,. \tag{A.3}$$

This simplified expression clearly shows that the theoretical error in R_K is very small even in the presence of NP. Note that in our numerical fit we have used the full expression of R_K with all the form factor dependent terms.

A.3 $B \to X_s\,\ell^+\,\ell^-$

The branching ratio for the inclusive decay $B \to X_s\,\ell^+\,\ell^-$ in the low-q^2 region can be written as [38]

$$\begin{aligned}\mathcal{B}(B \to X_s\ell^+\ell^-)_{[1,6]} = 10^{-7} \times \Big[&(15.86 \pm 1.51) + 2.663\, C_9^{\ell} - 0.049\, C_9^{\ell'} - 4.679\, C_{10}^{\ell} \\ &+0.061\, C_{10}^{\ell'} + 0.534\, (C_9^{\ell\,2} + C_9^{\ell'\,2}) + 0.543\, (C_{10}^{\ell\ 2} + C_{10}^{\ell'\,2}) \\ &-0.014\ C_9^{\ell} C_9^{\ell'} - 0.014\ C_{10}^{\ell} C_{10}^{\ell'}\Big]\,.\end{aligned} \tag{A.4}$$

We took the theoretical error into account by taking a gaussian prior for a parameter called b_0 and marginalizing over it, with its central value and standard deviation given by 15.86 and 1.51 respectively.

A.4 $B_s \to \ell^+\,\ell^-$

The branching ratio for the leptonic decays $B_s \to \mu^+\mu^-$ and $B_s \to e^+e^-$ can be written as

$$\mathcal{B}(B_s \to \mu^+\mu^-) = \mathcal{B}(B_s \to \mu^+\mu^-)_{\rm SM}\left|\frac{C_{10}^{\rm SM} + C_{10}^{\mu} - C_{10}^{\mu\,\prime}}{C_{10}^{\rm SM}}\right|^2 \tag{A.5}$$

$$\mathcal{B}(B_s \to e^+e^-) = 2.34 \times 10^{-5} \times \mathcal{B}(B_s \to \mu^+\mu^-)_{\rm SM}\left|\frac{C_{10}^{\rm SM} + C_{10}^{e} - C_{10}^{e\,\prime}}{C_{10}^{\rm SM}}\right|^2\,. \tag{A.6}$$

Here we have used the SM value of $\mathcal{B}(B_s \to \mu^+\mu^-)$ as our input parameter instead of the B_s meson decay constant f_{B_s} and the CKM matrix elements. We took the theoretical error on this into account by taking a gaussian prior for $\mathcal{B}(B_s \to \mu^+\mu^-)_{\rm SM}$ and marginalizing over it, using values from [23]:

$$\mathcal{B}(B_s \to \mu^+\mu^-)_{\rm SM} = (3.65 \pm 0.23) \times 10^{-9}\,.$$

JHEP12(2014)131

B Statistical procedure

In this appendix we briefly describe the statistical procedure that has been followed in this work. Our aim is to construct the posterior probability distributions (p.d.f.) for a set of WCs that we denote collectively by $\mathbf{C}$, for example $\mathbf{C} = \{C_9^\mu, C_9^e, \ldots.\}$.

The theoretical prediction for a given observable will be denoted by O and it will depend on $\mathbf{C}$ as well as a set of input parameters $\mathbf{x}$, for example CKM matrix elements, form factors, masses of the particles etc. The inputs are either experimentally measured quantities or theoretically calculated parameters with some uncertainties. In order to take into account these uncertainties we have to attach a probability distribution $f_{x_i}(x_i)$ to each input x_i.

The measured observables will be assumed to be distributed according to a Normal distribution with mean value $\overline{O}$ and standard deviation σ_O. The generalization to distributions other than the Normal distribution is straightforward.

If one has a set of N observables O_i $(i = 1, \ldots N)$, following the Bayesian approach,[1] the p.d.f. of the WCs can be written as

$$\rho\left(\mathbf{C}\right) \propto \int \prod_{i=1}^{N} \exp\left(-\frac{\left(O_i\left(\mathbf{C};\mathbf{x}\right) - \overline{O}_i\right)^2}{2\,\sigma_{O_i}^2}\right) \prod_j f_{x_j}(x_j) dx_j \ . \tag{B.1}$$

Let us now split the observables into two sets, O^+ and O^* where the second (first) set refers to the observables (without) involving the decay $B \to K^* \mu^+ \mu^-$. In a similar way, we split the set of inputs into three sets $\mathbf{x} = \{\mathbf{x}^+, \mathbf{x}^*, \mathbf{x^c}\}$ where $\mathbf{x}^+$ $(\mathbf{x}^*)$ are input parameters entering the set of observables O^+ (O^*) exclusively and $\mathbf{x^c}$ are the inputs which are common to both the sets of observables. The expression for the p.d.f. now reduces to

$$\begin{aligned}\rho\left(\mathbf{C}\right) \qquad \propto \int \prod_i \exp\left(-\frac{\left(O_i^+(\mathbf{C};\mathbf{x}^+,\mathbf{x^c}) - \overline{O_i^+}\right)^2}{2\,\sigma_{O_i^+}^2}\right) \times \prod_j \exp\left(-\frac{\left(O_j^*(\mathbf{C};\mathbf{x}^*,\mathbf{x^c}) - \overline{O_j^*}\right)^2}{2\,\sigma_{O_j^*}^2}\right) \\ \times \prod_{k_1} f_{x_{k_1}^+}(x_{k_1}^+) dx_{k_1}^+ \times \prod_{k_2} f_{x_{k_2}^*}(x_{k_2}^*) dx_{k_2}^* \times \prod_{k_3} f_{x_{k_3}^c}(x_{k_3}^c) dx_{k_3}^c \ .\end{aligned} \tag{B.2}$$

Now we would like to find the conditions such that the two sets of observables "factorize". In that case, we will be able to use the results of [3] instead of redoing the full analysis. The factorization is possible if the common set of inputs $\mathbf{x^c}$ has small uncertainty compared to the other sources of uncertainties. If that is true then one can write to a very good approximation $f_{x_k^c}(x_k^c) = \delta(x_k^c - \langle x_k^c \rangle)$ and the p.d.f. reduces to

$$\rho\left(\mathbf{C}\right) \propto \int \prod_i \exp\left(-\frac{\left(O_i^+\left(\mathbf{C};\,\mathbf{x}^+, \langle \mathbf{x^c} \rangle\right) - \overline{O_i^+}\right)^2}{2\,\sigma_{O_i^+}^2}\right) \times \rho_0\left(\mathbf{C}\right) \times \prod_j f_{x_j^+}(x_j^+) dx_j^+ \tag{B.3}$$

[1] In particular, in the same spirit of section 3 of [39].

JHEP12(2014)131

where $\rho_0\,(\mathbf{C})$ is the result of a Bayesian analysis considering only the global analysis of the decay $B \to K^* \mu^+ \mu^-$. Using the result of [3] in their section 3.2, we assume that

$$\rho_0\,(C_7, C_9^\mu) \propto \exp\left(-\frac{\left(C_7 - \overline{C_7}\right)^2}{2\,\sigma_{C_7}^2}\right) \exp\left(-\frac{\left(C_9^\mu - \overline{C_9^\mu}\right)^2}{2\,\sigma_{C_9^\mu}^2}\right) . \tag{B.4}$$

with

$$\overline{C_7} = -0.018\,, \quad \sigma_{C_7} = 0.018\,, \quad \overline{C_9^\mu} = -1.6\,, \quad \sigma_{C_9^\mu} = 0.3\,. \tag{B.5}$$

These values are inferred from eq. (4) of [3]. We finally remark that although ref. [3] considered the observable $\mathcal{B}\,(B \to X_s\,\ell^+\,\ell^-)$ under the assumption of lepton universality, we interpret that as $\mathcal{B}\,(B \to X_s\,\mu^+\,\mu^-)$ and remove the experimental data on $\mathcal{B}\,(B \to X_s\,\mu^+\,\mu^-)$ (our table 1) from our fit for consistency. We have also not used the data on $\mathcal{B}(B_s \to \mu^+\mu^-)$ since that was also already included in the fit of ref. [3].

C Input parameters

Parameters	Value	
G_F	1.166×10^{-5} GeV^{-2}	[25]
$\alpha_{em}(m_b)$	1/133	[25]
m_e	0.511 MeV	[25]
m_μ	105.6 MeV	[25]
$m_b(m_b)$	4.164 GeV	[37]
$m_{B^\pm}$	5.279 GeV	[25]
$m_{K^\pm}$	0.494 GeV	[25]
$\tau_{B^\pm}$	1.641×10^{-12} sec.	[25]
$\lvert V_{ts}^* V_{tb}\rvert$	40.58×10^{-3}	[40]
$m_{B_s^*}(1^-)$	5.366 GeV	[25]
Wilson coefficients		
$C_7^{\rm SM}(m_b)$	-0.319	[37]
$C_9^{\rm SM}(m_b)$	4.228	[37]
$C_{10}^{\rm SM}(m_b)$	-4.410	[37]
Form factors		
f_{BK}^+	$0.34^{+0.05}_{-0.02}$	[37]
f_{BK}^T	$0.39^{+0.05}_{-0.03}$	[37]
b_1^+	$-2.1^{+0.9}_{-1.6}$	[37]
b_1^T	$-2.2^{+1.0}_{-2.0}$	[37]

Table 5. Input parameters.

JHEP12(2014)131

References

[1] LHCb collaboration, *Differential branching fraction and angular analysis of the decay* $B^0 \to K^{*0}\mu^+\mu^-$, *JHEP* **08** (2013) 131 [arXiv:1304.6325] [INSPIRE].

[2] LHCb collaboration, *Measurement of form-factor-independent observables in the decay* $B^0 \to K^{*0}\mu^+\mu^-$, *Phys. Rev. Lett.* **111** (2013) 191801 [arXiv:1308.1707] [INSPIRE].

[3] S. Descotes-Genon, J. Matias and J. Virto, *Understanding the* $B \to K^*\mu^+\mu^-$ *anomaly*, *Phys. Rev.* **D 88** (2013) 074002 [arXiv:1307.5683] [INSPIRE].

[4] W. Altmannshofer and D.M. Straub, *New physics in* $B \to K^*\mu\mu$*?*, *Eur. Phys. J.* **C 73** (2013) 2646 [arXiv:1308.1501] [INSPIRE].

[5] R. Gauld, F. Goertz and U. Haisch, *On minimal* Z' *explanations of the* $B \to \mu^+\mu^-$ *anomaly*, *Phys. Rev.* **D 89** (2014) 015005 [arXiv:1308.1959] [INSPIRE].

[6] R. Gauld, F. Goertz and U. Haisch, *An explicit* Z'*-boson explanation of the* $B \to K^*\mu^+\mu^-$ *anomaly*, *JHEP* **01** (2014) 069 [arXiv:1310.1082] [INSPIRE].

[7] A. Datta, M. Duraisamy and D. Ghosh, *Explaining the* $B \to K^*\mu^+\mu^-$ *data with scalar interactions*, *Phys. Rev.* **D 89** (2014) 071501 [arXiv:1310.1937] [INSPIRE].

[8] A.J. Buras and J. Girrbach, *Left-handed* Z' *and* Z *FCNC quark couplings facing new* $b \to s\mu^+\mu^-$ *data*, *JHEP* **12** (2013) 009 [arXiv:1309.2466] [INSPIRE].

[9] A.J. Buras, F. De Fazio and J. Girrbach, 331 *models facing new* $b \to s\mu^+\mu^-$ *data*, *JHEP* **02** (2014) 112 [arXiv:1311.6729] [INSPIRE].

[10] W. Altmannshofer, S. Gori, M. Pospelov and I. Yavin, *Quark flavor transitions in* L_μ*-*L_τ *models*, *Phys. Rev.* **D 89** (2014) 095033 [arXiv:1403.1269] [INSPIRE].

[11] LHCb collaboration, *Test of lepton universality using* $B^+ \to K^+\ell^+\ell^-$ *decays*, *Phys. Rev. Lett.* **113** (2014) 151601 [arXiv:1406.6482] [INSPIRE].

[12] C. Bobeth, G. Hiller and G. Piranishvili, *Angular distributions of* $\bar{B} \to K\bar{l}l$ *decays*, *JHEP* **12** (2007) 040 [arXiv:0709.4174] [INSPIRE].

[13] G. Hiller and F. Krüger, *More model independent analysis of* $b \to s$ *processes*, *Phys. Rev.* **D 69** (2004) 074020 [hep-ph/0310219] [INSPIRE].

[14] S. Jäger and J. Martin Camalich, *On* $B \to Vll$ *at small dilepton invariant mass, power corrections and new physics*, *JHEP* **05** (2013) 043 [arXiv:1212.2263] [INSPIRE].

[15] J. Lyon and R. Zwicky, *Resonances gone topsy turvy — The charm of QCD or new physics in* $b \to s\ell^+\ell^-$*?*, arXiv:1406.0566 [INSPIRE].

[16] S. Descotes-Genon, L. Hofer, J. Matias and J. Virto, *On the impact of power corrections in the prediction of* $B \to K * \mu^+\mu^-$ *observables*, arXiv:1407.8526 [INSPIRE].

[17] R. Alonso, B. Grinstein and J.M. Camalich, SU(2) $\times$ U(1) *gauge invariance and the shape of new physics in rare* B *decays*, arXiv:1407.7044 [INSPIRE].

[18] G. Hiller and M. Schmaltz, R_K *and future* $b \to s\ell\ell$ *physics beyond the standard model opportunities*, *Phys. Rev.* **D 90** (2014) 054014 [arXiv:1408.1627] [INSPIRE].

JHEP12(2014)131

[19] C. Bobeth, G. Hiller and D. van Dyk, *General analysis of $\bar{B} \to \bar{K}^{(*)}\ell^+\ell^-$ decays at low recoil*, *Phys. Rev.* **D 87** (2013) 034016 [arXiv:1212.2321] [INSPIRE].

[20] LHCb collaboration, *Differential branching fraction and angular analysis of the $B^+ \to K^+\mu^+\mu^-$ decay*, *JHEP* **02** (2013) 105 [arXiv:1209.4284] [INSPIRE].

[21] T. Huber, E. Lunghi, M. Misiak and D. Wyler, *Electromagnetic logarithms in $\bar{B} \to X_s\ell^+\ell^-$*, *Nucl. Phys.* **B 740** (2006) 105 [hep-ph/0512066] [INSPIRE].

[22] BABAR collaboration, J.P. Lees et al., *Measurement of the $B \to X_s\ell^+\ell^-$ branching fraction and search for direct CP-violation from a sum of exclusive final states*, *Phys. Rev. Lett.* **112** (2014) 211802 [arXiv:1312.5364] [INSPIRE].

[23] C. Bobeth, et al., *$B_{s,d} \to \ell^+\ell^-$ in the standard model with reduced theoretical uncertainty*, *Phys. Rev. Lett.* **112** (2014) 101801 [arXiv:1311.0903] [INSPIRE].

[24] CMS and LHCb collaborations, *Combination of results on the rare decays $B^0_{(s)} \to \mu^+\mu^-$ from the CMS and LHCb experiments*, CMS-PAS-BPH-13-007 (2014).

[25] PARTICLE DATA GROUP collaboration, J. Beringer et al., *Review of particle physics*, *Phys. Rev.* **D 86** (2012) 010001 [INSPIRE].

[26] LHCb collaboration, *Observation of a resonance in $B^+ \to K^+\mu^+\mu^-$ decays at low recoil*, *Phys. Rev. Lett.* **111** (2013) 112003 [arXiv:1307.7595] [INSPIRE].

[27] HPQCD collaboration, C. Bouchard et al., *Standard model predictions for $B \to K\ell^+\ell^-$ with form factors from lattice QCD*, *Phys. Rev. Lett.* **111** (2013) 162002 [arXiv:1306.0434] [INSPIRE].

[28] HPQCD collaboration, C. Bouchard et al., *Rare decay $B \to K\ell^+\ell^-$ form factors from lattice QCD*, *Phys. Rev.* **D 88** (2013) 054509 [arXiv:1306.2384] [INSPIRE].

[29] R.R. Horgan, Z. Liu, S. Meinel and M. Wingate, *Lattice QCD calculation of form factors describing the rare decays $B \to K^*\ell^+\ell^-$ and $B_s \to \phi\ell^+\ell^-$*, *Phys. Rev.* **D 89** (2014) 094501 [arXiv:1310.3722] [INSPIRE].

[30] R.R. Horgan, Z. Liu, S. Meinel and M. Wingate, *Calculation of $B^0 \to K^{*0}\mu^+\mu^-$ and $B^0_s \to \phi\mu^+\mu^-$ observables using form factors from lattice QCD*, *Phys. Rev. Lett.* **112** (2014) 212003 [arXiv:1310.3887] [INSPIRE].

[31] S. Descotes-Genon, T. Hurth, J. Matias and J. Virto, *Optimizing the basis of $B \to K^*\ell^+\ell^-$ observables in the full kinematic range*, *JHEP* **05** (2013) 137 [arXiv:1303.5794] [INSPIRE].

[32] F. Beaujean, C. Bobeth and D. van Dyk, *Comprehensive bayesian analysis of rare (semi)leptonic and radiative B decays*, *Eur. Phys. J.* **C 74** (2014) 2897 [arXiv:1310.2478] [INSPIRE].

[33] A. Dighe, A. Kundu and S. Nandi, *Enhanced B_s -$\bar{B}_s$ lifetime difference and anomalous like-sign dimuon charge asymmetry from new physics in $B_s \to \tau^+\tau^-$*, *Phys. Rev.* **D 82** (2010) 031502 [arXiv:1005.4051] [INSPIRE].

[34] A. Dighe and D. Ghosh, *How large can the branching ratio of $B_s \to \tau^+\tau^-$ be?*, *Phys. Rev.* **D 86** (2012) 054023 [arXiv:1207.1324] [INSPIRE].

[35] A.K. Alok et al., *New physics in $b \to s\mu^+\mu^-$: CP-conserving observables*, *JHEP* **11** (2011) 121 [arXiv:1008.2367] [INSPIRE].

[36] A.K. Alok et al., *New physics in $b \to s\mu^+\mu^-$: CP-violating observables*, *JHEP* **11** (2011) 122 [arXiv:1103.5344] [INSPIRE].

JHEP12(2014)131

[37] A. Khodjamirian, T. Mannel, A.A. Pivovarov and Y.-M. Wang, *Charm-loop effect in $B \to K^{(*)}\ell^+\ell^-$ and $B \to K^*\gamma$*, *JHEP* **09** (2010) 089 [arXiv:1006.4945] [INSPIRE].

[38] S. Descotes-Genon, D. Ghosh, J. Matias and M. Ramon, *Exploring new physics in the C7-C7′ plane*, *JHEP* **06** (2011) 099 [arXiv:1104.3342] [INSPIRE].

[39] M. Ciuchini et al., *2000 CKM triangle analysis: a critical review with updated experimental inputs and theoretical parameters*, *JHEP* **07** (2001) 013 [hep-ph/0012308] [INSPIRE].

[40] CKMFITTER GROUP collaboration, J. Charles et al., *CP violation and the CKM matrix: assessing the impact of the asymmetric B factories*, *Eur. Phys. J.* **C 41** (2005) 1 [hep-ph/0406184] [INSPIRE], updated results and plots available at: http://ckmfitter.in2p3.fr.

JHEP12(2014)131